

The estimation of high density atmospheric motion vectors and their application to operational numerical weather prediction

J. Le Marshall, G. Mills, N. Pescod, R. Seecamp and K.K. Puri

Bureau of Meteorology Research Centre, Bureau of Meteorology, Australia

P. Stewart

National Meteorological and Oceanographic Centre, Bureau of Meteorology, Australia

L.M. Leslie

School of Mathematics, University of New South Wales, Australia

and

A. Rea

Observations and Engineering Branch, Bureau of Meteorology, Australia

(Manuscript received November 2001; revised July 2002)

As the spatial, temporal and spectral resolution of observations from space has improved, their benefit to numerical weather prediction (NWP) has increased. The utility of these data has also been aided by increased computer power, improved NWP models and the use of improving data assimilation techniques.

This paper provides a summary of high spatial and temporal resolution atmospheric motion vector (AMV) estimation at the Bureau of Meteorology and new data impact results for the Australian region. In particular, it summarises recent experiments examining the use of each type of these vectors in NWP and also details an operational trial in which all types of AMVs were used simultaneously. As a result of this trial, these AMVs are now used for operational regional NWP.

Introduction

Wind is a primary variable for describing atmospheric state. Accurate depiction of the wind field in areas with no conventional data is essential for operational weather forecasting and initialisation of NWP models. Measurement of wind from geostationary platforms is important as it provides near continuous data

where conventional observations are lacking, particularly over the data-sparse oceans. Studies as early as Bauer (1976) showed that AMVs have a capacity similar in several aspects to that of radiosondes for representing atmospheric flow.

Use of cloud-drift wind vectors is now widespread. Applications include nowcasting, global and regional NWP and tropical cyclone forecasting. The characteristics of the winds and their impact on medium-range global NWP was summarised in Kallberg et

Corresponding author address: Dr John Le Marshall, Bureau of Meteorology Research Centre, GPO Box 1289K, Vic. 3001, Australia.

al. (1982) and later by Kelly (1993), Kallberg and Uppala (1998) and Bouttier and Kelly (2001). Their impact in regional forecasts has been well documented, for example, in Le Marshall et al. (1992, 1993, 1994a, 1996a and 1999) and Velden (1996). The utility of AMVs for forecasting tropical cyclone tracks can be seen in Velden et al. (1984), Le Marshall et al. (1985), Velden et al. (1992, 1998), Velden (1997), Le Marshall et al. (1996b, 1996c), Leslie et al. (1998) and in Le Marshall and Leslie (1998). A summary of their impact for this application is also found in Le Marshall (1998).

This paper discusses recent regional data assimilation experiments and a related operational trial which successfully applied high resolution visible, infrared and water vapour band image-based motion vectors to operational regional NWP in the Australian Region.

AMV derivation at the Bureau of Meteorology

Estimation

The methods used for AMV estimation are largely covered in Le Marshall et al. (1994a, 1998, 1999). The imagery was navigated using orbit, attitude and landmark data from the documentation of the GMS-5 Stretched Visible and Infrared Spin Scan Radiometer (S-VISSR) transmission together with some refinements which included statistical correction of the navigation information to fit the landmark data and, on occasions, horizon detection. The system used three sequential infrared (IR), visible (VIS) or water vapour (WV) band images (a triplet), usually separated by an hour or half an hour for velocity estimation. The imagery was searched for potential target areas of 20 x 20 pixels (30 x 30 in the case of WV imagery) by examining maximum and minimum brightness temperature and gradient maxima. The size of the potential target areas for each wind type was determined by systematic testing.

Selected targets were tracked automatically using forecast winds, then a lagged correlation technique, which minimises root mean square (RMS) differences in brightness from successive pictures, was used to estimate the vector displacement.

Cloud height assignment for visible and IR targets used forecast temperature profiles. Determination of temperatures associated with various levels within the cloud and hence with the motion vectors used a number of methods. Initially, height assignment involved fitting Hermite polynomials to smooth raw histograms of brightness temperature. This enabled estimation of cloud base altitude from cloud base temperature using the forecast temperature profile. The

cloud height assigned for the low-level winds was that of the cloud base (following the field work of Hasler et al. 1976, 1977). The benefit of height assignment to the cloud base has been documented previously (Le Marshall and Pescod 1994).

Upper-level AMVs were assigned to the cloud top.

The cloud-top level was initially estimated by an examination of the cold tail of the upper cloud population, assuming the cloud temperature for the winds to be just above the coldest 5.5 per cent of the cloud population. The height assignment was based on the smoothed histograms, obtained from the Hermite polynomials, which were used to distinguish the contributions from high cloud as opposed to those from lower levels. The height assignment level for the AMVs moved from the estimated cloud base to the estimated level of the cloud top when it progressed from low to high cloud. A new system, using dynamic calibration, and 11 and 12 μm split window observations has been introduced into operations (Le Marshall et al. 1998). In this system, a check was made for the presence of transmissive cirrus at high levels and cloud top temperature was subsequently estimated using these two channels. Lower level heights were estimated, taking into account the effects of water vapour on brightness temperature, when calculating the cloud base temperature. These effects were estimated using the 11 and 12 μm split window observations. Another real time system has been under test using a 3-channel (11, 12 and 6.7 μm) algorithm with incorporation of the precise observation time for the AMV observations taken from various parts of the S-VISSR imagery, and improved quality control, particularly to prevent upper-level vectors being placed too low in the atmosphere during height assignment. In the case of water vapour motion vectors, the height assignment of the upper-level cloud vectors and middle-level vectors in clear conditions is described in Le Marshall et al. (1999).

Quality control

Wind data were accepted for assimilation and errors assigned based on several criteria. These included the correlation between the brightness temperature arrays of the search and target areas, and the differences in meridional and zonal wind components of the two vectors from a tracer tracked in pairs of adjacent images. The difference thresholds allowing use in the assimilation were situation dependent (near a jet stream, low level, etc.), and typically required the winds to be within 5 and 7 m s^{-1} for the zonal and meridional components respectively. The deviation of the calculated wind vectors from the first-guess field was also examined. The acceptable deviation was again situation dependent (near a jet stream, low

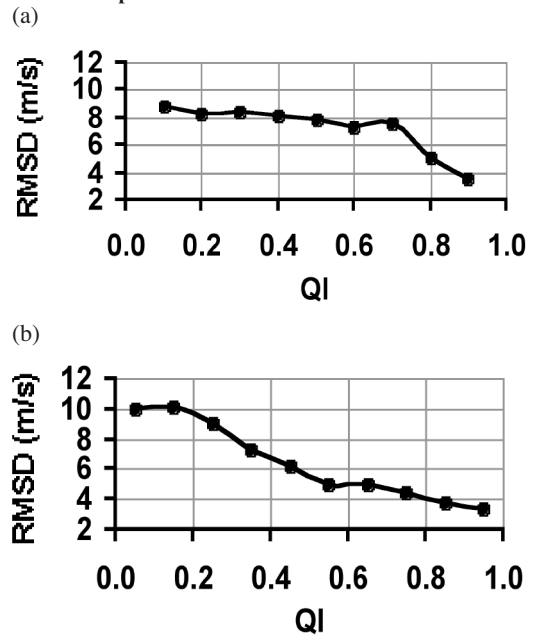
level, etc.) and zonal and meridional wind differences typically less than around 10 and 7 m s⁻¹ respectively, were required for inclusion in the assimilation.

The weights assigned to AMVs in the operational assimilation system are dependent on their level-dependent expected error. To enhance the use of AMVs in the assimilation, the quality control (qc) method cited above provided an expected error, based on previous collocation statistics generated from coincident radiosondes and AMVs. This allowed selection of vectors with errors appropriate to the assimilation system. It is important to note that the qc system is not static but changes, for example, with the assimilation system and the accuracy of the background field, i.e. changes, for instance, where the forecast model in the assimilation system is improved. As the accuracy of the background field improves, the ability to distinguish between reliable wind estimates and erroneous data is enhanced.

Recently, a Quality Indicator (QI) (Holmlund (1998) and Holmlund et al. (2001)), has been estimated and associated with each AMV in addition to the local error estimate. This gives AMV users some flexibility in quality control. The QI for each AMV is calculated by estimating direction consistency, speed consistency, vector consistency, spatial consistency and consistency with the operational forecast. These tests are similar in many ways to those employed above. The degree of compliance with these five tests is then used to form a single QI. The QI is intended to allow optimal use of high density winds, by giving a consistent estimation of the anticipated error associated with each vector. Using methods similar to Röhn et al. (1998), the QI has been provided for all AMV types generated at the Bureau of Meteorology (hereafter referred to as the Bureau).

Plots of QI versus rms difference between AMVs and radiosondes within 150 km, for both low-level infrared and high resolution visible AMVs, estimated

Fig. 1 Quality Indicator (QI) versus root mean square difference (RMSD) with radiosondes within 150 km for low level (a) infrared image based AMVs and (b) high resolution visible image based AMVs for 28 April 2000 to 29 April 2001.



using one years data (April 2000 – April 2001), are seen in Fig. 1. The QI information associated with the local AMVs is not currently used operationally in the Bureau, as quality control is still more efficient using local methods. That is, local methods currently provide more vectors with errors up to a given rms error level, than does use of the QI, employing currently published weights. Testing, however, is underway to tune the QI and to use it in conjunction with other quality measures such as the RFF (Holmlund et al. 2001).

Table 1. Cloud-drift wind types generated in the Bureau. The table indicates wind type, subsatellite image resolution, frequency of wind extraction, time of wind extraction and the separation of the image triplets used for wind generation (ΔT).

Wind type	Image resolution	Frequency/times (UTC)	Wind image triplet (ΔT)
IR	5 km	6 hourly - 05, 11, 17, 23	30 minutes
Low-res. VIS	5 km	6 hourly - 05, 23	30 minutes
High-res. VIS	1.25 km	6 hourly - 05, 23	30 minutes
Water Vapour	5 km	6 hourly - 05, 11, 17, 23	30 minutes
IR (hourly)	5 km	Hourly - 00, 01, 02, ... 23	1 hour
Low-res. VIS (hrly)	5 km	Hourly - 00, 01, 02, ... 23	1 hour
High-res. VIS (hrly)	1.25 km	Hourly - 00, 01, 02, ... 23	1 hour
Water Vapour (hrly)	5 km	Hourly - 00, 01, 02 ... 23	1 hour

It should be noted that, if QI rather than the expected error is to be used globally, then calibration curves (see Fig. 1) need to be estimated for each vector type or an internationally consistent (normalised) QI is needed. (i.e. the same QI means similar error characteristics for all AMV types from different providers). It may, however, be simpler to provide the expected error with each AMV, as is under test in the Bureau.

Accuracy

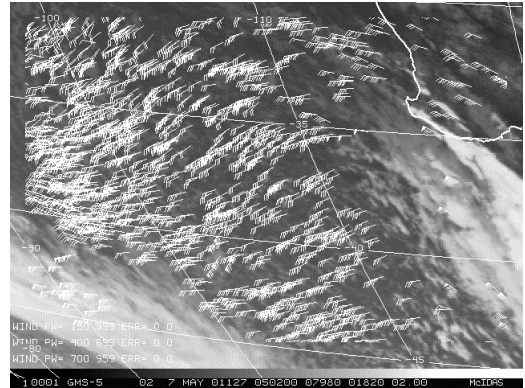
The wind types generated by the Bureau's operational Australian region forecast system and their characteristics are listed in Table 1.

A selection of winds, estimated by the operational AMV system is shown in Fig. 2. The local IR ($11\ \mu\text{m}$) system alone can provide up to 400 wind vectors around Australia at 05, 11, 17 and 23 UTC. Each individual vector generated by the system is provided to the user, not an average of the two vectors generated by each image triplet. This may be significant when the data are assimilated at the observation time (as in 4-D Var). The accuracy of the local wind system during a recent operational trial described in the next section is seen in Table 2 which shows the mean modulus of the vector deviation (MMVD) of the AMVs from radiosondes within 150 km for the period 12 September to 30 October 2000 over the Australian region.

AMVs in regional NWP

In earlier data assimilation experiments over the Australian region, different types of local AMVs were added individually to the Bureau's operational data base to gauge their impact on regional NWP (Le Marshall et al. 1994a, 1996a, 1999). After the completion of these experiments, all vectors have been used together with the Bureau's real time database in

Fig. 2 Local cloud and water vapour AMVs southwest of Australia for 0500 UTC on 7 May 2001.



an operational trial to gauge their combined impact on regional NWP.

The first three experiments examined the impact of infrared ($11\ \mu\text{m}$), hourly and water vapour ($6.7\ \mu\text{m}$) imagery based winds on operational forecasts. They employed a duplicate near real-time Limited Area Prediction System (LAPS) (Puri et al. 1998), identical to the operational real-time system except for the addition of real time test AMVs to the input data. The data were inserted at six-hourly intervals. The data base to which these AMVs were added already contained local TOVS data (Le Marshall et al. 1994b), any JMA winds available at the operational cut-off time (+6 h for the 0600 and 1800 UTC based forecasts and + 1.5 h for the 1200 and 0000 UTC based forecasts), and, in some cases (e.g. the addition of hourly and water vapour based winds), local $11\ \mu\text{m}$ infrared cloud-drift winds.

Table 2. Comparison of radiosonde and atmospheric motion vectors using CGMS (Coordination Group for Meteorological Satellites) criteria, 12 September – 30 October, 2000. [IR1 = $11\ \mu\text{m}$ imagery based winds, VIS. = Low resolution (5 km) visible winds, HR VIS. = High resolution (1.25 km) visible winds, WV = Water Vapour based winds and MMVD = mean magnitude of vector difference (m s^{-1})]

Type		IR1	VIS.	HR VIS.	WV
Low (950 – 700 hPa)	No. of obs.	500	190	994	---
	MMVD (m/s)	3.33	3.49	3.33	---
Middle (699 – 400 hPa)	No. of obs.	8	---	6	254
	MMVD (m/s)	6.46	---	5.38	5.44
High (399 – 150 hPa)	No. of obs.	622	116	398	1896
	MMVD (m/s)	5.79	6.45	5.51	6.34

The assimilation methodology

The analyses on which the forecasts reported here are based start with a global analysis (Seaman et al. 1995), valid 12 hours prior to the forecast start time. This is used as a first guess to the regional analysis, which then provides the base analysis for an initialised six-hour forecast, a subsequent analysis and a further initialised six-hour forecast. This forecast is then used as a first guess to the final analysis from which the 24 and 48-hour forecasts are run. Forecasts are nested in fields from the most recent Bureau of Meteorology global model forecast (Bourke et al. 1995).

The analysis and forecast models

The LAPS analysis and forecast model for the first three experiments used a common latitude/longitude/sigma coordinate system. The configuration consisted of 160 x 110 grid-points at 0.75° spacing in the horizontal, and 19 levels in the vertical, with an upper level of sigma 0.05. The analysis system was a limited area adaptation of the global multivariate statistical interpolation analysis. The errors assigned to the AMVs in the operational analysis scheme are 3 m s⁻¹, 4 m s⁻¹ and 5 m s⁻¹ for low, middle and high level vectors respectively. This is consistent with the 3 m s⁻¹ errors assigned to middle and high level radiosonde observations and the differences between collocated AMVs and radiosonde wind estimates recorded at the Bureau. They are consistent with the differences for the period shown in Table 2. The forecast model is described in Puri et al. (1998) and is a hydrostatic model formulated in latitude/longitude/sigma coordinates on the Arakawa A-grid. It uses high order numerics and includes a comprehensive physics package and digital filter initialisation.

Earlier studies: application of infrared (11 μm) based winds in the Australian region. This study gauged the impact of local six-hourly GMS-5 IR1 AMV data on operational NWP in the Australian Region (Le Marshall et al. 1996a). The local AMV system provided winds at six-hourly intervals from triplets of half-hourly GMS-5 IR1 (10.1 - 11.7 μm) imagery. LAPS was employed with six-hour cycling and the operational database to provide the control forecasts. In parallel, using the same assimilation system, the local IR1 AMVs were added to the operational data base for real-time assimilation runs. The S1 skill scores (Teweles and Wobus 1954), tabulated on the official National Meteorological and Oceanographic Centre (NMOC) verification grid, for 24-hour forecasts from the local AMV (LAPS + IR)

Table 3(a). Twenty-four hour forecast verifications (S1) for the operational regional model (LAPS) and LAPS with local GMS-5 IR1 AMVs (LAPS + IR) for 20 June to 18 August 1995 (19 cases).

Level	(LAPS)S1	(LAPS + IR)S1
MSLP	26.4	25.4
850 hPa	24.8	23.9
500 hPa	16.1	15.7
300 hPa	14.0	13.7

Table 3(b). Twenty-four hour forecast verifications (S1) for the control (LAPS) and the control plus hourly/six-hourly IR and VIS AMVs (LAPS + VIS/IR-Hrly) for 5 September to 4 December 1995 (22 cases)

Level	(LAPS + IR)S1	(LAPS + VIS/IR-Hrly) S1
MSLP	27.6	26.7
850 hPa	29.2	27.7
500 hPa	19.0	18.7
300 hPa	16.6	16.1

Table 3(c). Twenty-four hour forecast verification (S1) for the control (LAPS) and LAPS with water vapour motion vectors (LAPS + WV) for March 1998 (33 cases)

Level	(LAPS) S1	(LAPS + WV) S1
MSLP	25.2	25.1
850	25.9	25.4
500	20.1	19.4
300	17.3	16.8

and matching control forecasts (LAPS) are shown in Table 3(a). The local AMVs have a consistent positive impact on the forecasts (around one skill-score point near the surface), a result consistent with that found for GMS-4 (Le Marshall et al. 1994a).

Application of hourly IR and hourly and six-hourly VIS in the Australian region. A second experiment (Le Marshall et al. 1996a) used hourly IR and VIS winds added to the (operational) control data base (which now included local six-hourly IR winds). Winds generated from image triplets centred within one hour of analysis time were used. Differences resulting from the use of these hourly winds were evident in the resulting analyses. The S1 skill scores for the 24-hour control forecasts (LAPS) and for the matching forecasts with VIS and IR AMVs (LAPS + VIS/IR-Hrly) are shown in Table 3(b). These indicate

that the additional winds have the potential to improve operational NWP even when six-hourly local IR AMVs were in the control data base. The main impact was a gain of around one skill-score point in the lower troposphere.

The application of water vapour AMVs in the Australian region. In this real-time experiment (Le Marshall et al. 1999), AMVs calculated four times per day from 30-minute triplets of water vapour images, were added to the operational database and used in a parallel forecast system. Thirty three forecasts were examined and the results are summarised in Table 3(c). In much of the region, particularly over the oceans, the water vapour winds provide the majority of the upper and middle-level AMVs and usually led to a small but discernible change in the analysed fields. Table 3(c) shows that the addition of water vapour motion vectors to the operational database provided on average, at all levels examined, a modest improvement in the twenty-four hour regional forecasts. In particular cases, however, the improvement can be quite significant, for example, up to five points during this trial. In some cases, water vapour motion vectors can clearly be seen to contain important information for analysis.

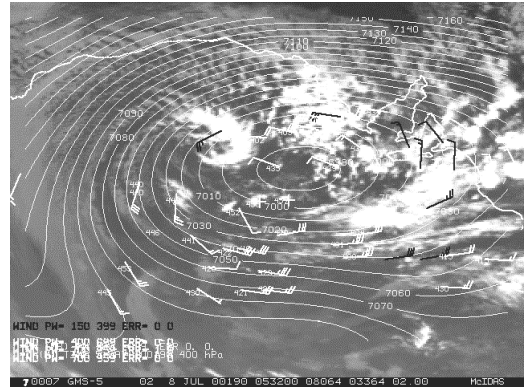
Figure 3, for example, shows a GMS-5 water vapour image for 0530 UTC on 8 July 2000 overlaid by the operational 400 hPa analysis for the same time. In this case, water vapour AMVs indicate that the low centre in the operational analysis at 400 hPa, which had no access to these data, should be further to the south west.

The operational trial

Here we provide recent results from a significant real-time experiment, where all the AMV types (infrared, visible and water vapour image based AMVs) in the previous experiments were added to the operational regional assimilation system (already containing IR1 winds). The methodology was that in the previous three experiments. There were, however, some changes in the assimilation system, in particular, a move from 0.75° to 0.375° horizontal resolution and 19 to 29 vertical levels.

The accuracy of the real-time AMVs used in this experiment in late 2000 is summarised in Table 2 which shows the mean magnitude of vector difference for different wind types compared to radiosondes within 150 km. Local quality control methods were used to provide vectors with expected errors consistent with the error levels used for AMVs in the operational analysis, namely 3 m s^{-1} , 4 m s^{-1} and 5 m s^{-1} for low, middle and high-level vectors respectively.

Fig. 3 GMS-5 water vapour AMVs with pressure heights displayed over an 0530 UTC GMS-5 $6.7 \mu\text{m}$ image on 8 July 2000 with the NMOC 400 hPa analysis for the same time.



The statistics in Table 2 correspond to an expected rms difference (error) threshold in the case of lower level IR1 winds, of around 4 m s^{-1} (or a QI threshold of 0.83). The data insertion methodology used for this operational trial is summarised in Fig. 4 which shows winds generated from triplets of IR, VIS and HR VIS images, with the images separated by one or half an hour, have been used when the image triplet is centred within one hour of the analysis time. In the case of winds generated from WV imagery, only winds generated from the triplet of images, separated by 30 minutes at the analysis time were used. This approach provided AMV coverage and accuracy, consistent with the resolution and characteristics of the data assimilation system.

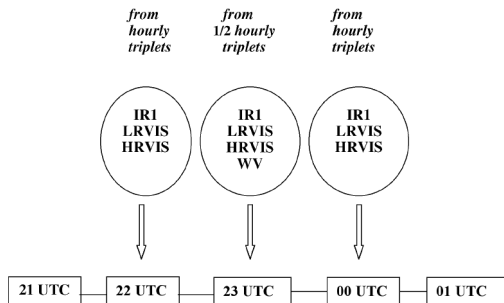
The S1 skill-scores for 24-hour forecasts from using these data are compared to the operational skill scores in Table 4. The statistics are consistent with those recorded in the three earlier experiments.

The results of this real time experiment are also illustrated in Figs 5 and 6. Figure 5 shows that the

Table 4. Twenty-four hour forecast verification (S1) for the operational regional forecast system (LAPS) and LAPS with VIS, IR and WV, hourly image based AMVs for 12 September - 30 October 2000 (47 cases).

LEVEL	(LAPS) S1	(LAPS + VIS/IR/WV HRLY) S1
MSLP	25.6	24.6
850 hPa	24.8	24.2
500 hPa	16.6	16.5
300 hPa	14.7	14.5

Fig. 4 Schematic diagram showing the nominal central image time of triplets used to generate wind estimates (AMVs) in the experimental assimilation of VIS/HRVIS, WV and IR1 image-based winds.



addition of these data has improved the real-time forecasts at all levels with greater impact in the lower troposphere. Figure 6 shows the daily S1 skill score gain at MSLP. It is clear these winds are beneficial to the forecast process.

In summary, these real-time IR, VIS, HRVIS and WV image based AMVs, are of an accuracy which can benefit operational regional NWP. Addition of the vectors individually to the operational regional forecast system has resulted in forecast improvements. The use of the AMVs together has provided both improved data coverage of the region and also resulted in forecast improvement.

As a consequence of this trial, all of these wind types have been employed in the operational regional forecast system in NMOC, Melbourne since October 2000.

Summary and conclusions

The local estimation of real-time operational AMVs and their impact on regional NWP has been described. Experiments using these data individually and together in an operational NWP trial have been summarised. The benefit of these data to operational regional NWP has been clearly recorded. These results have led to the introduction of all these wind types into NMOC's operational database and their use in operational regional NWP since October 2000.

In relation to the future, the continuing trend to space-based observations with higher spatial, temporal and spectral resolution should enable improved estimation of atmospheric motion and result in quantitative benefit to NWP. In particular, the prospects of significant benefits from the use of sequential obser-

Fig. 5 Skill scores (12 Sept to 30 Oct 2000) from 47 cases for NMOC forecasts (OPS) and OPS with vis/IR/WV AMVs (OPS/AMV) for (47 cases).

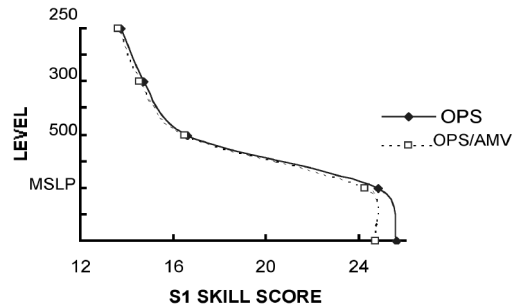
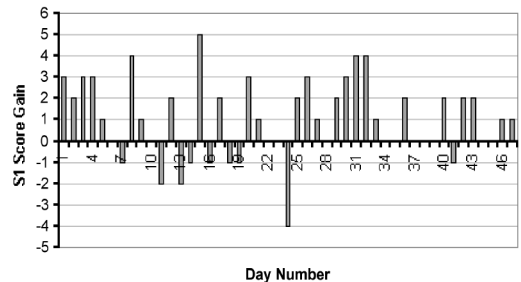


Fig. 6 Skill score gain for 24 h forecasts at MSLP with use of the VIS, IR and WV AMVs (12 September - 30 October 2000).



vations from MTSat-1R, FY-2 and new generation ultra-spectral instruments such as the Geostationary Imaging Fourier Transform Spectrometer (Smith et al. 2000) appear to be very good.

Acknowledgments

Thanks are due to Terry Adair and Irene Mouzouri for assistance in the preparation of this manuscript.

References

Bauer, K.G. 1976. Comparison of cloud motion winds with coinciding radiosonde winds. *Mon. Weath. Rev.*, 104, 922 - 31.
 Bourke, W.P., Hart, T., Steinle, P., Seaman, R., Embery, G., Naughton, M. and Rikus, L. 1995. Evolution of the Bureau of Meteorology's Global Assimilation and Prediction System. Part 2: Resolution enhancements and case studies. *Aust. Met. Mag.*, 44, 19 - 40.

- Bouttier, F. and Kelly, G. 2001. Observing system experiments in the ECMWF 4D-VAR data assimilation system. *Q. Jl R. Met. Soc.*, 127, 1469 - 88.
- Hasler, A.F., Shenk, W. and Skillman, W. 1976. Wind estimates from cloud motions: Phase I of an in situ aircraft verification experiment. *Jnl appl. Met.*, 15, 10 - 15.
- Hasler, A.F., Shenk, W. and Skillman, W. 1977. Wind estimates for cloud motions: preliminary results of phase I, II and III of an in situ aircraft verification experiment. *Jnl appl. Met.*, 16, 812 - 15.
- Holmlund, K. 1998. The Utilization of Statistical Properties of Satellite-derived Atmospheric Motion Vectors to Derive Quality Indicators. *Weath. Forecasting*, 13, 1093 - 1104.
- Holmlund, K., Velden, C. and Röhn, M. 2001. Enhanced automatic quality control applied to high-density satellite derived winds. *Mon. Weath. Rev.*, 129, 517 - 29.
- Kallberg, P.S., Uppala, S., Gustafsen, N. and Palleaux, J. 1982. The Impact of Cloud Drift Wind Data on Global Analysis and Medium Range Forecasts, *ECMWF Technical Note Number 34*, 55p, (Available from ECMWF, Shinfield Park, Reading, Berkshire RG2 9AX, United Kingdom).
- Kallberg, P. and Uppala, S. 1998. Impact of Cloud Motion Winds on the ECMWF ERA 15 Reanalyses. *Proc. Fourth International Winds Workshop*, Saanenmoser, Switzerland, 20 - 23 October, 1998. EUM P 24, ISSN 1023-0416, 109 - 106.
- Kelly, G. 1993. Numerical experiments using cloud motion winds at ECMWF. *Proceedings of the Second International Winds Workshop*. Tokyo, Japan. 13-15 December, 1993. Published by EUMETSAT EUM P14. ISSN 1023-0416, 227 - 244.
- Le Marshall, J., Smith, W. and Callan, G. 1985. Hurricane Debby - An illustration of the complementary nature of VAS soundings and cloud and water vapour drift winds. *Bull. Am. Met. Soc.*, 66, 258 - 63.
- Le Marshall, J.F., Pescod, N.R., Mills, G.A. and Stewart, P.K. 1992. Cloud drift winds in the Australian Bureau of Meteorology: An operational note. *Aust. Met. Mag.*, 40, 247 - 50.
- Le Marshall, J.F., Pescod, N.R. and Allen, G. 1993. The real-time generation and application of cloud drift winds in the Australian region. *Aust. Met. Mag.*, 42, 89 - 103.
- Le Marshall, J.F., Pescod, N., Seaman, R., Mills, G. and Stewart, P. 1994a. An Operational System for Generating Cloud Drift Winds in the Australian Region and Their Impact on Numerical Weather Prediction. *Weath. Forecasting*, 9, 361 - 70.
- Le Marshall, J.F., Riley, P.A., Rouse, B.J., Mills, G.A., Wu, Z.-J., Stewart, P.K. and Smith, W.L. 1994b. Real-time assimilation and synoptic application of local TOVS raw radiance observations. *Aust. Met. Mag.*, 43, 153 - 66.
- Le Marshall, J.F. and Pescod, N. 1994. Generation and application of cloud drift winds in the Australian Region - recent advances. *Proceedings of the Pacific Ocean Remote Sensing Conference*, Melbourne, Australia, 1 - 4 March, 1994, 467 - 74.
- Le Marshall, J.F., Spinoso, C., Pescod, N.R. and Mills, G.A. 1996a. Estimation and assimilation of hourly high spatial resolution wind vectors based on GMS-5 observations. *Aust. Met. Mag.*, 45, 275-84.
- Le Marshall, J.F., Leslie, L.M. and Spinoso, C. 1996b. The impact of spatial and temporal distribution of satellite observations on tropical cyclone data assimilation: Preliminary results. *Met. Atmos. Phys.*, 60, No. 1 - 3, 157 - 63.
- Le Marshall, J.F., Leslie, L.M. and Bennett, A.F. 1996c. Tropical Cyclone Beti, an example of the benefits of assimilating hourly satellite wind data. *Aust. Met. Mag.*, 45, 275 - 9.
- Le Marshall, J.F. 1998. Cloud and Water Vapour Motion Vectors in Tropical Cyclone Track Forecasting - A Review. *Met. Atmos. Phys.*, 65, 141 -51.
- Le Marshall, J.F. and Leslie, L.M. 1998. Tropical cyclone forecasting using cloud drift winds and a new methodology. *Aust. Met. Mag.*, 47, 261 - 6.
- Le Marshall, J.F., Pescod, N., Seecamp, R., Spinoso, C. and Rea, A. 1998. Improved Weather Forecasts from Continuous Generation and Assimilation of High Spatial and Temporal Resolution Winds. *Proc. Fourth International Winds Workshop*, Saanenmoser, Switzerland, 20 - 24 October, 1998, 101 - 108.
- Le Marshall, J.F., Pescod, N., Seecamp, R., Puri, K., Spinoso, C. and Bowen, R. 1999. Local estimation of GMS-5 water vapour motion vectors and their application to Australian region numerical weather prediction. *Aust. Met. Mag.*, 48, 73-7.
- Leslie, L.M., Le Marshall, J.F., Morison, R.P., Spinoso, C., Purser, J., Pescod, N. and Seecamp, R. 1998. Improved hurricane track forecasts from the continuous assimilation of high quality satellite wind data. *Mon. Weath. Rev.*, 126, 1248-58.
- Puri, K., Dietachmeyer, G., Mills, G.A., Davidson, N.E., Bowen, R.M. and Logan L.W. 1998. The new BMRC Limited Area Prediction System, LAPS. *Aust. Met. Mag.*, 47, 203 - 23.
- Röhn, M., Kelly, G. and Saunders, R. 1998. Transition to cloud motion winds from Meteosat with 90 minute sampling and the use of the MPEF quality indicator. *EUMETSAT/ECMWF Research Report No. 7*.
- Seaman, R., Bourke, W., Steinle, P., Hart, T., Embery, G., Naughton, M. and Rikus, L. 1995. Evolution of the Bureau of Meteorology's Global Assimilation and Prediction system. Part 1: analysis and initialisation. *Aust. Met. Mag.*, 44, 1 - 18.
- Smith, W.L., Harrison, F.W., Revercomb, H.E., Bingham, G.E., Huang H.L. and Le Marshall, J.F. 2000. The Geostationary Imaging Fourier Transform Spectrometer. *Proc. Eleventh International TOVS Study Conference*, Budapest, Hungary. 391 - 8.
- Teweles, S. and Wobus, H. 1954. Verification of prognostic charts. *Bull. Am. Met. Soc.*, 35, 455 - 63.
- Velden, C.S., Smith, W.L. and Mayfield, M. 1984. Application of VAS and TOVS to Tropical Cyclones. *Bull. Am. Met. Soc.*, 65, 1059 - 67.
- Velden, C.S., Hayden, C.M., Menzel, W.P., Franklin, J.L. and Lynch, J.S. 1992. The impact of satellite-derived winds on numerical hurricane track forecasting. *Weath. Forecasting*, 7, 107 - 18.
- Velden, C.S. 1996. Winds derived from geostationary satellite moisture channel observations: applications and impact on numerical weather prediction. *Met. Atmos. Phys.*, 60, 37 - 46.
- Velden, C.S., Hayden, C.M., Nieman, S.J., Menzel, W.P., Wanzong, S. and Goerss, J.S. 1997. Upper tropospheric winds derived from geostationary satellite water vapor observations. *Bull. Am. Met. Soc.*, 78, 173 - 95.
- Velden, C.S., Olander, T.L. and Wanzong, S. 1998. The impact of multispectral GOES-8 wind information on Atlantic tropical cyclone track forecasts in 1995, Part 1. Dataset methodology, description and case analysis. *Mon. Weath. Rev.*, 126, 1202 - 18.